First Middle East Conference on Smart Monitoring,
Assessment and Rehabilitation of Civil Structures
8 – 10 February 2011, Dubai, UAE

SMAR 2011

High-resolution 3D condition survey of a masonry arch bridge using Ground Penetrating Radar

A. Kalogeropoulos[1], E. Brühwiler[1]

[1] EPFL, Ecole Polytechnique Fédérale de Lausanne, Lausanne, Switzerland

ABSTRACT: Condition surveying is essential before rehabilitation and modification of a structure. It implies information collection and analysis for structural performance evaluation. Common condition surveying often requires obstructive and invasive techniques that can affect the structure's integrity. Also, the extent of internal disorders and their distribution in the structure is not obtained. The use of non-destructive techniques combined with external analysis, can provide useful information for structural condition surveying.

This paper presents the application of Ground Penetrating Radar for the condition survey of a massive natural stone masonry bridge with twin large span arches. Emphasis is placed on the determination of the condition of the arches. The paper describes the processing steps leading to a high-resolution 3D reconstitution of spatial and structural information for disorder mapping. Benefits and limits of this novel representation method for massive bridge structures will be reviewed.

1 INTRODUCTION

A 110 year old massive natural stone masonry arch bridge shows signs of cleavage emerging on the inner side face of its two main arches. Cleavage may affect the bearing capacity of the arch structure depending of their quantity and extent. The degree of cleavage was not known with accuracy. The provision of high-resolution spatial information on the main arches of the bridge was required in order to determine the extent of cleavage, and subsequently to check the structural safety. The use of Ground Penetrating Radar (GPR) was proposed as an investigation tool for its ability to locate the presence of structural disorders, like cracks, in detailed and continuous dataset.

The objective of this study is to conduct a high-resolution 3D mapping, using GPR datasets, locate cleavages and their magnitude in the sandstone masonry rings forming the main arches of the bridge.

2 THE BRIDGE

The historical bridge located in Central Europe carries four lanes of road traffic plus two pedestrian footpaths. It is composed of twin parallel principal arches having a 85m span and a clearance of 42 meters. The structure is surmounted by 8 smaller arches. The reinforced concrete bridge deck is 150 meters long and 17 m wide.

2.1 Arches

The primary arches are composed of three interlocking rings (Fig. 1) of voussoirs. Each voussoir is composed of seven blocks of dolomitic sandstone masonry, each one having a width of about 30 cm, being 90 cm long and having an alternating thickness (crenulation) of 60 and 90 cm. The connection between the blocks is ensured with lime mortar.

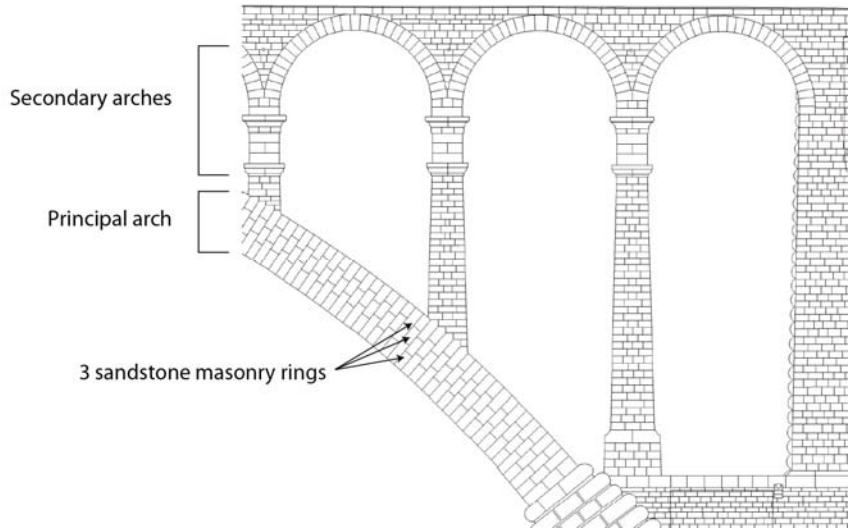

Figure 1. Structure of the bridge arches

2.2 Disorders

During periodic condition surveys of the structure, thin cracks with openings smaller than 1mm at the surface and emerging on the inside face of the arches were observed (Fig. 2). Moreover, evidence of water circulation was present on the intrados and the side faces of the arches.

Figure 2. Emerging cracks on the arches inner side face

3 GROUND PENETRATING RADAR

3.1 Principle

GPR is a Non Destructive method that sends electromagnetic pulses and records their variation. It produces datasets (profiles) relating the structure of investigated objects. The datasets are composed of a series of measurements (traces) along a line. A trace is a recording of the variation of electric potential in time, of electromagnetic pulses propagating and reflecting within the material (Fig. 3).

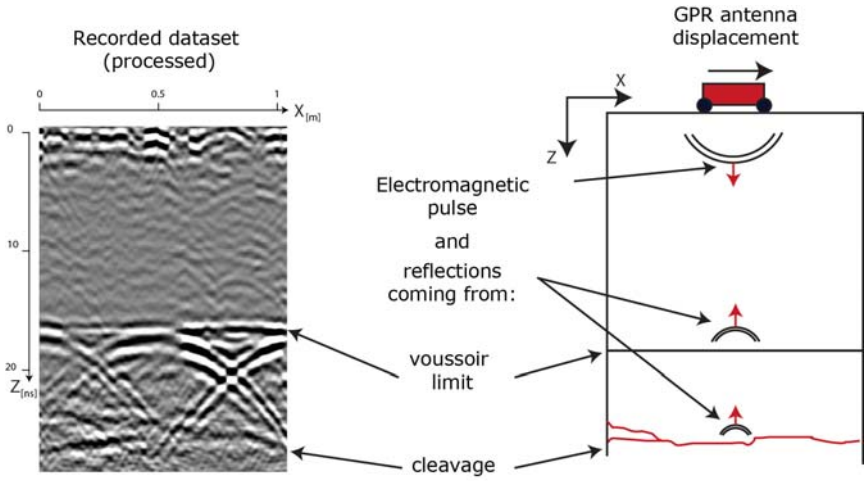

Figure 3. GPR principle

3.2 Electromagnetic parameters

Electromagnetic waves consist of variations of an electric field **E** and a magnetic field **H** that are perpendicular one to each other and to the direction of propagation of the wave. In a dielectric medium the velocity of electromagnetic waves depends on the conductivity and the dielectric permittivity. Conductivity (σ) is the capacity of the media to conduct electrical currents. Dielectric permittivity (ε) can be seen as the rebound capacity of the media after an electromagnetic stimulation. Interface laws (Snell's law) state that for every propagating wave, a constant describing the reflection depends on the angle of incidence of the wave and on the ratio between the velocities of propagation within the two media. As each material has its own permittivity and conductivity, an electromagnetic wave emitted by a GPR antenna will propagate at different velocities in each type of material (air, stone, and water). In this way a reflection is occurring at each interface between two different materials (Fig. 3).

3.3 Technical aspects

GPR antennas are defined by their centre frequency. This corresponds to the peak of the energy distribution following frequencies. The centre frequency is used as a reference, because it gives an indication of the resolution (size of detectable objects) and the range of investigation that can be covered. The choice of the centre frequency is a compromise between depth of investigation and the resolution. The depth of investigation is increasing at lower centre frequencies, and the resolution is increasing at higher centre frequencies.

The resolution depends also on the electromagnetic parameters of the investigated material (σ and ε), for that reason a calibration measurement must be carried out before measurements to ensure the maximum depth of investigation and the detectability of the objects of interest.

4 MEASUREMENTS

4.1 Calibration

The calibration phase consists of comparing antennas with two different centre frequencies 900 MHz and 1.5 GHz. A limited portion of one of the arch intrados presenting cracks on its side face is used as a reference site. The calibration has three purposes: first to find the most efficient balance between depths of investigation and resolution; second, to determine data acquisition direction, parallel or perpendicularly to the blocks; and third, estimate electromagnetic waves propagation velocity in sandstone.

4.1.1 Antenna selection

The 900 MHz centre frequency antenna provides a maximum depth of investigation of 1.5 m and has poor capacity to detect cleavages. The 1.5 GHz centre frequency antenna provides exploitable information within a range of 1 m to 1.2 m and allows detecting a cleavage of about one millimetre. With this sufficiently efficient balance the 1.5 GHz centre frequency antenna is selected for the rest of the study.

4.1.2 Data acquisition direction

Two different directions of acquisition are tested, the first one perpendicular to the blocks and the second parallel (Fig. 4). The first direction of acquisition concludes that the block width (30 cm) is too small, and is generating a lot of scattering in the datasets. With this it was not possible to detect the layer of cleavage. While the second acquisition direction provides good results the blocks length being of 90 cm, only little scattering is generated. This scattering is due to the spherical spreading of electromagnetic waves. It is related to λ the wavelength of the pulse emitted by the antenna in the considered media.

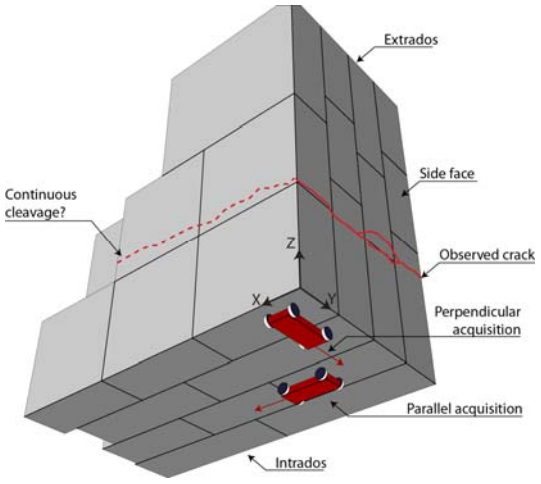

Figure 4. GPR calibration setup

4.1.3 Wave velocity estimation

Velocity estimation is essential; it links the time of arrival of recorded electromagnetic waves with the depth of the reflectors. The travel time is twice the distance multiplied by the wave velocity. It takes into account that the travelled distance is double. The wave emitted from the antenna travels to the interface, is reflected and propagates back to the receiver.

A reference site showing no cracks on the inner side face of the arch is selected to avoid any disturbance. The velocity estimation is performed using the common mid-point technique: two antennas are placed at equal distance from a central point. The distance between the antennas is decreased simultaneously until both antennas reach the centre point. The measured velocity is 0.12 m/ns. This velocity value can be compared with the hyperbolic shapes observed at the bottom of the blocks reflections. Theses hyperbolas (Fig. 5) correspond to the reflections from the sides of the blocks, moving away and approaching the GPR displacement. The intersection of the hyperbolas correspond to the centre of the blocks, the antenna is then equidistant to each side. The shape of the hyperbolas is linked to the wave velocity, fitting them provides an estimation of the wave velocity in the material. The estimated velocity was equal to the one measured with the common mid-point technique.

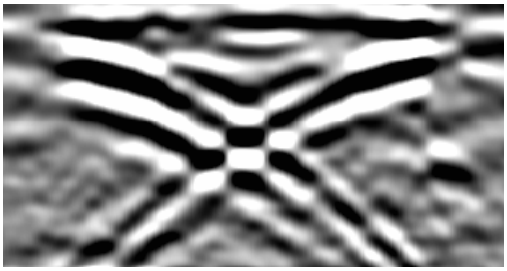

Figure 5. Hyperbolic reflections coming from the sides of the blocks

4.2 Measurement campaign

The measurement campaign was conducted over a period of 10 days. A total amount of 384 GPR profiles were recorded. The profiles were recorded principally from the intrados of the arches. When it was possible measurements were performed from the extrados of the arches. The measurements required the use of a positive lift platform, a negative lift platform, and an access point on the extrados of the arches.

4.2.1 Data processing

To enhance interpretation, the recorded profiles must be treated with signal processing techniques. The trace is normalised with the correction of the Dc shift. The low frequency noise is removed with Dewowing. Constant reflections are removed with background removal. The amplitude of the lower reflections is increased by multiplying traces with gain functions. Multiples are removed using spiking deconvolution. Noise is removed with f-k filtering. These different signal processing procedures are described in detail within GPR literature, (D.J. Daniels).

5 RESULTS

After processing, the profiles interpretations are assembled into a scaled 3D representation, based on photogrammetric 2D plans provided by Archeotech. Areas identified as possibly showing cleavages are identified on each profile. They are linked from one profile to another depending on the depth of the damage detected. The obtained cleavage areas are therefore an extrapolation from profile to profile. They are an approximation of the actual state of the bridge. With this it is possible to distinguish three levels of cleavage shown in Fig. 6.

- One level of cleavage (green) was found between 0.4 and 0.6 m from the extrados of the arches in the centre of the upper ring.

- A second level of cleavage (red) was found between 0.7 and 0.9 m from the intrados of the bridge, this level corresponds to the limit of the mortar joint between the lower ring and the central ring.

- The last level of cleavage (yellow) was found between 0.4 and 0.6 m from the underside of the bridge into the lower ring.

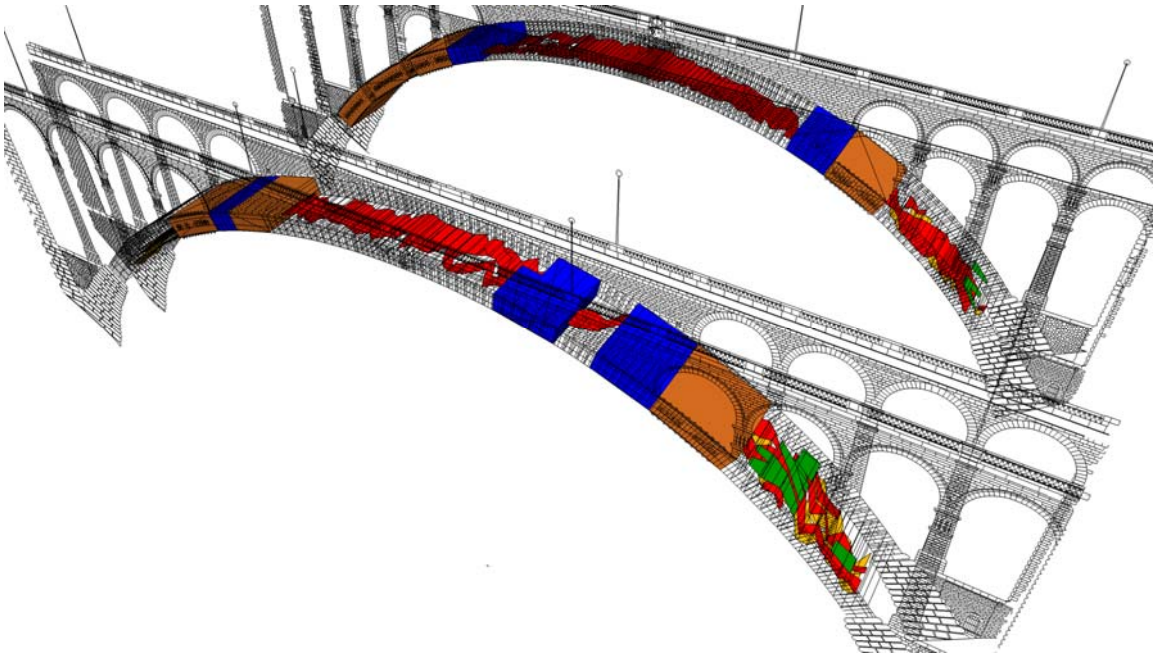

Figure 6.3D output of interpreted disorders on the principal arches of the bridge.

The brown areas indicate the zones where data was not collected. In addition, it must be specified that the depth of penetration of radar is ranging between 1 to 1.2 m and the arches are 3 meters thick, consequently there is only little or no information on the centre ring of the arch.

5.1 Additional information

5.1.1 Border effects

The first and last centimetres of each profile could not be interpreted. Similar to the edges of blocks generating hyperbolic reflections, the spandrel walls of the arches create a significant interference (reflection) masking underlying reflections from possible cleavage.

5.1.2 Water damping

Some profiles show damping generated by changes in the electromagnetic parameters of the material. This is due to the presence of water and/or chlorides in the masonry. This damping is estimated by comparing the amplitudes of two reflectors located at the same depth with the direct wave present in all GPR datasets (Table 1).

Table 1.Signal damping due to the presence of water and/or chlorides

Profile type	Direct wave amplitude	Reflector amplitude	Damping in dB
Dry	2032	656	-9.82
Wet	2032	64	-30.034

In most of the cases this damping can be compensated with gain functions. But some profiles suffering too much damping couldn't as the noise is superior to signal; in such cases the profile is indicated in blue on the cartography.

5.1.3 Verification

Based on data from the cartography, a range of 14 boreholes have been drilled and their respective cores analysed. A comparison between the fractures observed on the cores and GPR datasets has confirmed the presence of cleavage. In general the boreholes indicate a larger amount of cleavage than the ones detected with GPR.

6 CONCLUSIONS

A 3D cartography of the extent and depth of cleavages was produced using GPR results combined with complementary investigation. It was observed that several levels of cleavage are present in the main arches of the bridge. Finally, some areas are identified having presence of water and/or chlorides in the masonry. Further work would assess the changes in water content contained in masonry blocks, based on analysis of the damping of radar signals.

References

Adey, B., Hajdin, R., Brühwiler, E. 2003.Supply and demand system approach to the development of bridge management strategies, Journal of Infrastructure Systems, ASCE, Vol. 9, Nr 3, pp. 117-131, 2003.

Brühwiler, E., Adey, B.: Improving the consideration of life-cycle costs in bridge decision-making in Switzerland. Journal of Structure and Infrastructure Engineering, Taylor & Francis, Vol. 1, No 2, June 2005, pp 145-158.

Daniels, D.J. (2004). Ground Penetrating Radar (2nd Edition). Institution of Engineering and Technology.

Hugenschmidt; J, and Mastrangelo, R. 2006. GPR inspection of concrete bridges. Cement and Concrete Composites. Volume 28, Issue 4: 384-392

Diamanti, N,Giannopoulos, A, and C. Forde, M. 2008. Numerical modeling and experimental verification of GPR to investigate ring separation in brick masonry arch bridges. NDT & E International, Volume 41, Issue 5: 354-363

Battista, MB, Addison, AD, and Knapp, CC. 2009. Empirical Mode Decomposition Operator for Dewowing GPR Data, J. Environ. Eng. Geophysics 14, 163 (2009); doi:10.2113/JEEG14.4.163

Grandjean, A., Brühwiler, E. 2009. Load-bearing capacity of masonry arch bridges using a plastic model. Protection of Historical Buildings, Rome, 21-24 June, 2009.

Hugenschmidt, J,and Kalogeropoulos, A. 2009. The inspection of retaining walls using GPR. Journal of applied geophysics, Journal of Applied Geophysics, Volume 67, Issue 4, April 2009, Pages 335-344, ISSN 0926-9851, DOI: 10.1016/j.jappgeo.2008.09.001

Hugenschmidt, J., Kalogeropoulos, A., Soldovieri, F., Prisco, G. 2010. NDT & E International, Volume 43, Issue 4, June 2010, Pages 334-342, ISSN 0963-8695, DOI: 10.1016/j.ndteint.2010.02.002.